

## PRODUCTION TECHNOLOGY DEVELOPMENT OF NiTi SMA BY ELECTRON BEAM MELTING

**Eduardo Massao Sashihara, emassao@ita.br**

Instituto Tecnológico de Aeronáutica, Praça Mal. Eduardo Gomes 50, 12228-900, S. J. dos Campos, SP, Brazil

**Daniel Soares de Almeida, dsa62@yahoo.com**

Instituto de Aeronáutica e Espaço, Praça Mal. Eduardo Gomes 50, 12228-900, S. J. dos Campos, SP, Brazil

**Odair Doná Rigo, odair@ctmsp.mar.mil.br**

Instituto Tecnológico de Aeronáutica, Praça Mal. Eduardo Gomes 50, 12228-900, S. J. dos Campos, SP, Brazil

**Jorge Otubo, jotubo@ita.br**

Instituto Tecnológico de Aeronáutica, Praça Mal. Eduardo Gomes 50, 12228-900, S. J. dos Campos, SP, Brazil

**Abstract.** *This work shows the importance of some processing parameters such as EB power, EB exposure time and raw material feeding speed on the production of NiTi SMA by Electron Beam Melting. They were produced three ingots, all presenting smooth and shiny surface indicating no oxidation. Depending upon the EB current intensity the resulting ingot presented rough columnar grains or finer columnar + equiaxed grains. The weight loss varied from 0.5% to 1.2% depending upon the EB current. It is also shown in this work that the production of NiTi SMA is perfectly possible as far as certain cares are taken into account.*

**Keywords:** *NiTi, Electron Beam Melting, Shape Memory Effect.*

### 1. INTRODUCTION

The NiTi alloys possess one of the best performance in terms of Shape Memory Effect (SME) and Pseudoelastic Effect (PE) with shape recovery up to 8%, and besides they are fatigue and corrosion resistant, highly biocompatible and have excellent vibration damping capacity (Loeb et al. 1994; Stoeckel, 1989). Therefore, these alloys have a wide range of technological and medical applications (Duerig, 2002; McGowan, 2002; Otsuka and Wayman, 1998).

However, their production and mechanical processing are not easy tasks due to mainly the contamination by carbon and oxygen which induce material brittleness and modify the martensitic transformation temperatures when produced by the conventional Vacuum Induction Melting (VIM). The alternative Electron Beam Melting (EBM) process for the production in large scale of this high purity alloy is considered pioneer in the world, with the contaminants content (carbon and oxygen) lower than the usual VIM process. Moreover, the difficulty of controlling the nominal chemical composition due to the high vacuum operation which causes some component evaporation has been overcome (Otubo et al. 2005, 2004, 2003 and 1998; Cruz et al. 2004). Before of this, only Matsumoto (1991a, 1991b) produced some small samples of NiTi alloy using EBM.

The aim of this work was to develop the processing technique of the NiTi Shape Memory Alloy (SMA) by EBM obtaining ingots whose macro and microstructures were characterized by optical microscopy (OM) and scanning electron microscopy (SEM). Complementary methods as hardness testing, differential scanning calorimetry (DSC) and/or energy dispersive spectroscopy (EDS) were necessary to establish relations with some EB parameters.

The NiTi samples produced here would be Ni-rich superelastic at room temperature. Some solution and/or ageing treatments were accomplished in as-cast condition to verify the formation of the precipitates within the NiTi matrix that theoretically influence the SME and PE.

### 2. EXPERIMENTAL PROCEDURES

The experimental procedures can be described as the production of three cylindrical ingots (CYL-1, CYL-2 and CYL-3) by **Continuous Feeding** the rod charge (Ni+Ti) and **Static Ingot Casting** into a constant volume cylindrical water-cooled copper crucible with 34mm (bore diameter) by 40mm (height) using 30kW EB furnace with chamber internal pressure better than  $5.0 \times 10^{-2}$ Pa. The EB melting bath originating from one single EB gun has a diameter of 25mm with +/-5mm deflection along the X/Y directions.

The starting raw materials were: 99.95% purity electrolytic nickel (bars of 4.3mm diameter and sheets of 1.0mm thick) and 99.56 to 99.7% purity grade 1 titanium (bars of 5.1mm diameter and sheets of 0.4mm thick).

For the production of the CYL-1 and CYL-2 ingots, the feeding rods were prepared by intercalating nickel bars with titanium bars encased into a two U-shaped titanium sheets, as can be seen in Fig.1. The total weight of the feeding rods for the both CYL-1 and CYL-2 ingots were 287.0g and 313.8g, respectively. A minimum length of approximately 250mm of the feeding rod was estimated for the purpose to fill the total crucible volume of the 24,740mm<sup>3</sup> and a 16.4x16.6 mm<sup>2</sup> cross-section area was taken into account to reduce feeding rod shadow in the melting pool and also to avoid dripping off the liquid outside the crucible of 34mm in diameter.

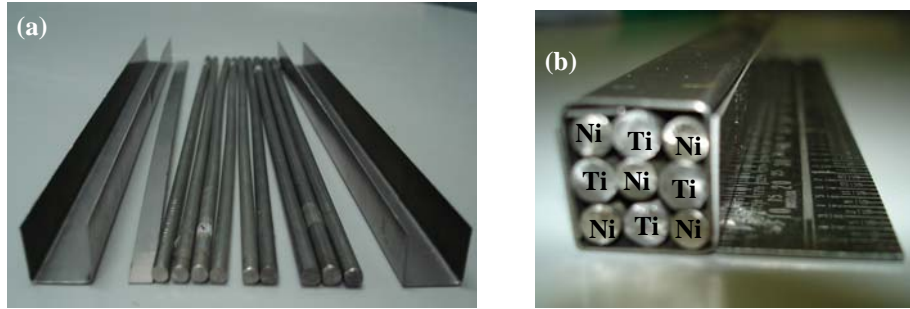


Figure 1. (a) Disposed raw materials before mounting and (b) after mounting of feeding rods for the CYL-1 and CYL-2.

For the CYL-3 ingot, instead of Ti and Ni bars they were used Ti sheets ( $0.4 \times 20 \times 270 \text{mm}^3$ ) intercalated with Ni sheets ( $1.0 \times 20 \times 270 \text{mm}^3$ ), resulting in total cross-section of  $\sim 13 \times 20 \text{mm}^2$ . Before melting, the set (382.1g) was consolidated by EB welding using 0.1A current on the two lateral position.

All the feeding charges have a nominal composition along the length of Ti56.0wt%Ni.

Table 1 presents the processing parameters (EB current and rod charge feeding speed and rotation) applied for each ingot.

Table 1. EBM processing parameters.

Ingot	EB current (A)	Rod charge feeding speed ( $\text{mm min}^{-1}$ )	Rod charge rotation (rpm)
CYL-1	0.5 – 0.6	23.0	3.0
CYL-2	1.0 – 1.2	10.0	3.0
CYL-3	0.8 – 1.0	10.0	zero

In accordance with Table 1, the processing parameters were intentionally modified although the ingots would have equals composition and dimensions (CYL-1, CYL-2 and CYL-3).

After the melting step, the EB current was slowly decreased until shoot down to avoid contraction cavity and the ingots were kept under vacuum for at least 30 minutes before the pressurization and chamber opening. The ingots were weighted before and after the melting in order to check the elements losses. More details of the production methods can be seen in the reference of Sashihara (2007).

Among the above ingots, only the CYL-1 and CYL-2 ingots (in as-cast, solution treated and/or in an aged conditions) were characterized by OM, SEM, hardness testing, DSC and/or EDS analysis, as required, in order to relate microstructural characteristics, hardness, transformation temperatures and/or composition control along the ingot to the processing parameters such as EB power and melting rate.

For the macro analysis, the ingots were initially cut by Discotom-6 Struers cut-off machine (speed of  $0.1 \text{mm sec}^{-1}$  and diamond wheel), and their surfaces were properly grinded up to sandpaper #400 and chemically attacked in a solution of  $94\% \text{H}_2\text{O} + 5\% \text{HNO}_3 + 1\% \text{HF}$ .

For the hardness testing, the ingots surfaces were grinded up to sandpaper #1200 and mechanically polished up to  $1 \mu\text{m}$ . The hardness testing were done with the Süsslen-Wolpert hardness-meter (150kg load and diamond headed cone) and with the Digital Microhardness Tester FM, Future-tech (300gf load and 8sec indentation time).

For the microstructural and EDS analysis, the ingots surfaces were grinded up to sandpaper #1200, mechanically polished up to  $1 \mu\text{m}$  and chemically attacked in a solution of  $94\% \text{H}_2\text{O} + 5\% \text{HNO}_3 + 1\% \text{HF}$ , as required. A microscope Zeiss DSM950 was used (secondary electrons and work voltage of 20kV). The phases volume fraction results were calculated by Image Tool software, average of 5 measurements with standard deviation of 6.0 max.

The DSC analysis was done using the Netzsch DSC-404C equipment. The samples were cut by Isomet-1000 (500rpm and 250g) with diamond wheel in order to minimize the material deformation. All the thermal cycle was done in helium gas atmosphere with following steps: a heating from 25 to  $100^\circ\text{C}$  at  $5^\circ\text{C}/\text{min}$ , a plateau at  $100^\circ\text{C}$  for 10min, a cooling from 100 to  $-80^\circ\text{C}$  at  $5^\circ\text{C}/\text{min}$ , a plateau at  $-80^\circ\text{C}$  for 10min and a second heating up to  $100^\circ\text{C}$  at  $5^\circ\text{C}/\text{min}$ .

### 3. RESULTS AND DISCUSSION

Under the visual aspect, all the ingots presented smooth and shiny surface and almost no oxidation was observed (sufficient cooling time under vacuum).

Table 2 shows the general physical data of the ingots and total weight loss during their EBM processing.

Table 2. NiTi Ingots physical data and total weight loss.

Ingot	Dimensions (mm)	Weight (g)	Total Weight Loss g/ (%)
CYL-1	Ø ~30; height ~42	181.4	6.2/ (3.3)
CYL-2		194.5	2.3/ (1.2)
CYL-3		235.7	1.2/ (0.5)

According to Table 2, the total weight loss was higher for the CYL-1 ingot due to the occurrence of unusual stirring of the melt during melting. For the CYL-2 and CYL-3 ingots, the total weight losses were due only to components evaporation with maximum of 2.3g or 1.2% for the first. This weight loss value has been reduced for the CYL-3 ingot probably due to decrease of the EB current, as shows the Tab.1.

Let's start analyzing as-cast CYL-1 and CYL-2 ingots in terms of macrostructures and hardness profiles. It makes known that the hardness values are apparent and serve only as a indication because the nominal composition of both ingots are in a superelastic state with the possibility of strain recovery upon load release.

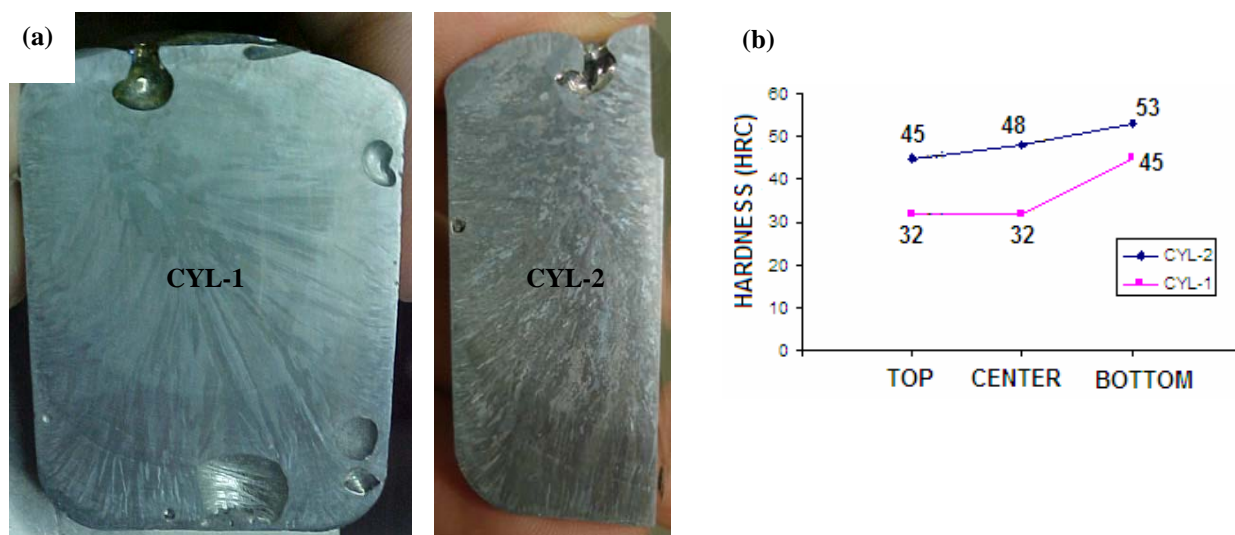


Figure 2. (a) Macrostructures and (b) hardness profiles of the as-cast CYL-1 and CYL-2 ingots.

As can be seen in Fig.2(a), the CYL-1 ingot presented some regular and round voids near to mold wall with smooth and shiny surface suggesting the gas formation although the EBM process has been done upon vacuum. Further, its grain structure can mostly be described by columnar crystals. For the other hand, the CYL-2 ingot presented no internal voids and its grain structure is composed by two typical zones: columnar grains elongated parallel to the direction of maximum heat transfer and equiaxed grains centrally located on the top with finer grains. Consequently, as shown in Fig.2(b), the hardness value of CYL-2 ingot is higher than that of the CYL-1 ingot. Besides, the hardness values of both ingots increase from top to bottom in opposition to solidification direction, Figure 2(b), respecting the ingot bottom has been rapidly cooled by larger contact area with the water-cooled copper crucible promoting finer microstructure.

Figure 3 shows the microstructure of the as-cast CYL-2 ingot (for as-cast CYL-1 ingot, the images are similar). The precipitates ( $TiNi_3$ ,  $Ti_2Ni$  or  $Ti_4Ni_2O$ ) are arranged within the NiTi matrix, as detailed: intermittent and clustered lamellas (in the top and center) or else larger and dispersed spherical-shaped (in the bottom).

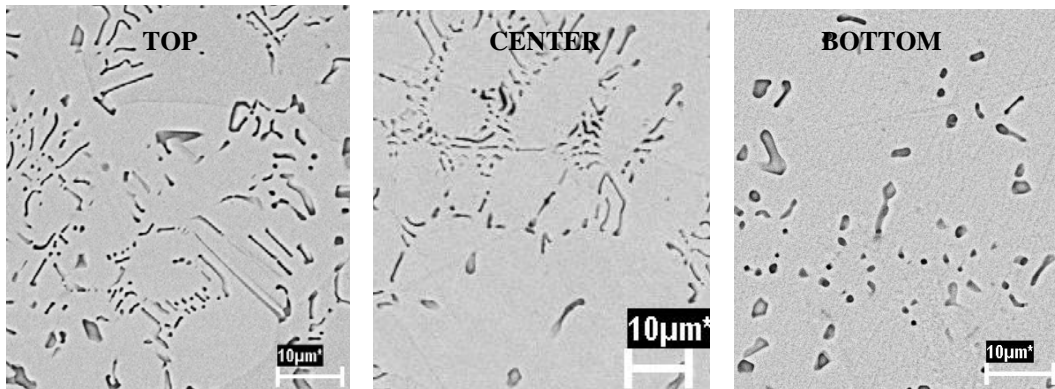


Figure 3. Microstructure of the as-cast CYL-2 ingot, transversal sections (top, center and bottom), by SEM (2000x). Attack in solution of 94% H<sub>2</sub>O + 5% HNO<sub>3</sub> + 1% HF.

The phases volume fraction results of the as-cast CYL-1 and CYL-2 ingots are compared in Fig.4. The as-cast CYL-2 ingot has a bit more precipitates than the as-cast CYL-1 ingot along the length probably due to the higher EB current and lower feeding speed promoting longer exposure time for the first. Besides, both ingots have less precipitates at the bottom probably due to higher cooling rate in this region.

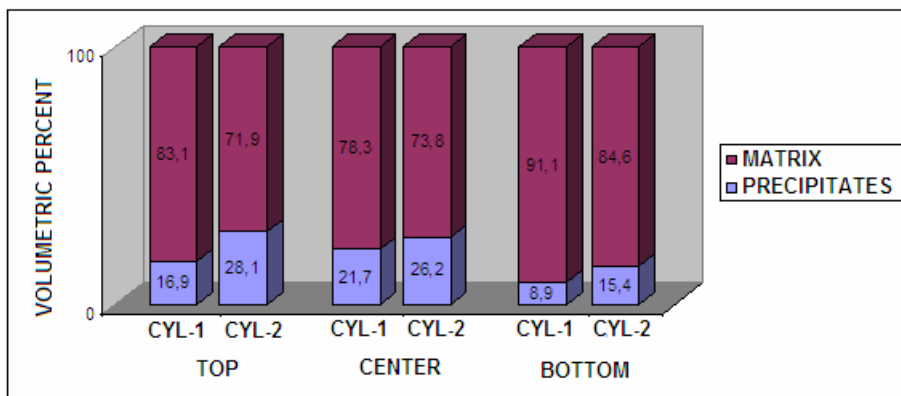


Figure 4. Phases volume fraction results of the as-cast CYL-1 and CYL-2 ingots, transversal sections (top, center and bottom). Software: Image Tool, average of 5 measurements with standard deviation of 6.0 max.

According to literature, if the EB exposure time is increased and higher the EB current, the more superheating, and therefore the more melting fluidity, in such a way it improves the surface and structural aspects of the ingots. However, the weight loss due to components evaporation can deviate the nominal chemical composition (Vassileva et al. 2005 and 2001; Koleva et al. 2001; Mitchell, 1999; Dietrich and Stephan, 1998). Besides, during the CYL-1 and CYL-2 ingots processing, it has been observed that the U-shaped external titanium case melts before the melting of internal nickel and titanium bars upon the EB incidence. According to NiTi Phases Diagram, the near-equiatomic alloy starts solidification at 1310°C (congruent point). In spite of the titanium melting point be higher than that of the nickel, the anticipated melting of the U-shaped titanium case especially occurs due to the direct EB incidence on the small thickness Ti sheets. In addition, the temperature of the liquidus line decreases from pure element to near-equiatomic composition more rapidly in the Ti-rich side, reaching eutectic temperature of 942°C as soon as the intermetallic compound starts to form. The consequence is the formation of pellet of low melting point in the feeding bar tip, as can be seen in Fig.5(a) promoting the sequence of pelletisation and dropping off the melt as the feeding proceeds. At first, this event can also contribute for the deviation of the nominal composition.

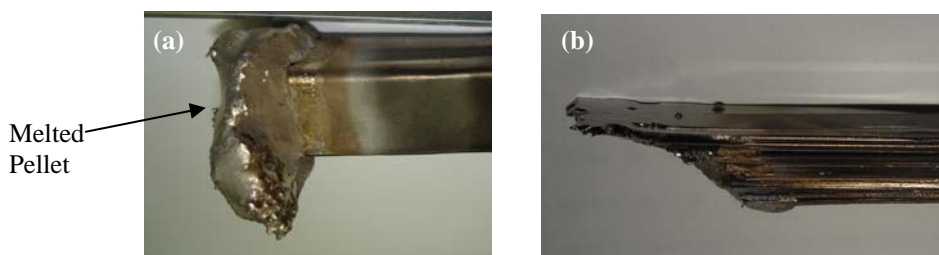


Figure 5. (a) CYL -1 ingot remaining feeding rod with melted pellet (for the CYL-2 ingot is similar), and (b) CYL-3 ingot Remaining Feeding Rod.

Table 3 presents the approximated chemical composition obtained by EDS analysis upon the NiTi matrix and precipitates in the top, center and bottom along its axis.

Table 3. Approximated chemical composition of the as-cast CYL-2 ingot, by EDS analysis.

Ingot Position	Component	NiTi Matrix wt % (at %)	Precipitates wt % (at %)
Top	Ti	44.45 (49.52)	44.63 (49.70)
	Ni	55.55 (50.48)	55.37 (50.30)
Center	Ti	44.21 (49.27)	44.30 (49.36)
	Ni	55.79 (50.73)	55.70 (50.64)
Bottom	Ti	43.86 (48.91)	44.83 (49.90)
	Ni	56.14 (51.09)	55.17 (50.10)

Owing to small total weight loss of 2.3g and compositional fluctuations (Tab.3) for the as-cast CYL-2 ingot, it is supposed that this ingot has good compositional homogeneity along the axial direction, so that both the NiTi matrix and precipitates have near-equiatomic composition. Besides, the decrease in nickel content from the bottom to top along the ingot axis (Tab.3) is intimately related to the casting configuration used (Otubo et al. 2003). Nevertheless, the posterior DSC analysis at same ingot revealed no martensitic transformation temperature at all indicating a certain deviation from the nominal composition of Ti56.0wt%Ni.

The modification of the CYL-3 ingot feeding rod to a intercalated Ni+Ti sheets and reduction of EB current along with no rotation of feeding rod promoted continuous dripping of the melt avoiding pelletization and also lower weight loss of 0.5% compared to 1.2% of CYL-2. The aspect of the remaining feeding rod of the CYL-3 ingot is shown in Figure 5(b) and can be compared to Figure 5(a), the feeding rods of the ingots CYL-1 and CYL-2. The CYL-3 ingot will be characterized in the future with the research development.

It should be emphasized that in the **Continuous Feeding** and **Static Ingot Casting**, (in the EB furnace used), the homogenization is difficult due to some aspects such as: small melting pool volume in relation to total volume, difficulty to produce an uniform EB density over the pool due to lack of EB control and the appearance of the feeding rod shadow over the melting pool and its level raising as the casting proceeds. When the pool level is near to crucible bottom, its exposure to the EB is lower minimizing the Ni evaporation. As the pool level increases, the intensity of the incident EB increases thereby increasing component evaporation, mainly nickel with higher vapour pressure (Vassileva et al. 2005 and 2001; Otubo et al. 2003; Koleva et al. 2001; Mitchell, 1999; Dietrich and Stephan, 1998).

#### 4. CONCLUSIONS

In this work, three NiTi SMA ingots were produced by EBM varying the processing parameters and main results are summarized below.

All the ingots presented smooth and shiny surface and almost no oxidation.

The total weight loss values were 1.2% for CYL-2 and 0.5% for CYL-3 ingots. The weight loss decrease was due to lowering the EB current.

The CYL-1 ingot presented mainly rougher columnar structure compared to CYL-2 ingot which presented finer columnar and equiaxed grains. Consequently the second ingot presented no voids, higher hardness values and higher volume fraction of precipitates.

Although the EDS analysis suggests a good compositional homogeneity for CYL-2 ingot, the DSC analysis revealed no martensitic transformation temperatures indicating composition deviation from the nominal one. This fact could be attributed to the formation of the melted pellet on the tip of the feeding rod.

The change of feeding rod configuration to an intercalated Ni+Ti sheets promoted continuous dripping of the melt.

Concluding, this work showed that the production of NiTi SMA by EBM is possible as has been shown by others works of the group.

## 5. ACKNOWLEDGEMENTS

To FAPESP grants 04/13131-7 and 00/09730-1.

To CTA-IAE-AMR; ITA; FATEC-SP; MACKENZIE; SULTRADE/STRÜERS; IPEN and POLI-USP for the laboratorial facilities.

## 6. REFERENCES

Cruz, L.A.F., Otubo, J., Moura Neto, C., Rigo, O.D., Mei, P.R., 2004, "Produção e caracterização de lingote da liga NiTi com Efeito de Memória de Forma", 10° Encontro de Iniciação Científica e Pós-Graduação – ENCITA, 19-20 Outubro de 2004, ITA, S. J. dos Campos, São Paulo, Brazil.

Dietrich, W., Stephan, H., 1998, "Electron Beam Melting and Casting", ASM Handbook, Vol. 15, pp. 410-419.

Duerig, T.W., 2002, "The use of superelasticity in modern medicine", MRS Bulletin, Vol. 27, No. 2, pp. 101-104.

Koleva, E., Vutova, K., Mladenov, G., 2001, "The role of ingot-crucible thermal contact in mathematical modelling of the heat transfer during electron beam melting", Vacuum, Vol. 62, pp. 189-196.

Loeb, B., Oliveira, J.F., Mendes, M., Sakima, T., Barreau, G., 1994, "Desenvolvimento de ligas com memória de forma", Revista ABM Metalurgia e Materiais, Vol. 50, No. 431, pp. 692-698.

Matsumoto, H., 1991a, "Addition of an element to NiTi alloy by an electron-beam melting method", Journal of Materials Science Letters, Vol. 10, pp. 417-419.

Matsumoto, H., 1991b, "Possibility of preparation of multicomponent samples by electron-beam melting", Journal of Materials Science Letters, Vol. 10, pp. 596-597.

Mcgowan, A.M.R., 2002, "Industrial and commercial applications of smart structures technologies", Proceedings of Spie: The International Society for Optical Engineering, San Diego, USA, 18-21 March, 2002.

Mitchell, A., 1999, "The electron beam melting and refining of titanium alloys", Materials Science and Engineering A, Vol. 263, pp. 217-223.

Otsuka, K., Wayman, C.M., 1998, "Shape Memory Materials", New York: Cambridge University Press, 289 p.

Otubo, J., Mei, P.R., Koshimizu, S. and Martinez, L.G., 1998, "NiTi shape memory alloys produced by electron beam melting: preliminary results", The Minerals, Metals & Materials Society, TMS, Vol. 1, pp. 1063-1068.

Otubo, J., Rigo, O.D., Moura Neto, C., Kaufman, M.J. and Mei, P.R., 2003, "Scale up of NiTi shape memory alloy production by EBM", Journal of Physique, IV France, Vol. 112, pp. 873-876.

Otubo, J., Rigo, O.D., Moura Neto, C., Kaufman, M.J. and Mei, P.R., 2004, "Low carbon content NiTi shape memory alloy produced by electron beam melting", Materials Research, Vol. 7, No. 2, pp. 263-267.

Otubo, J., Rigo, O.D., Moura Neto, C. and Mei, P.R., 2005, "The effects of VIM and EBM processing techniques on the purity of NiTi SMA", International Conference on Martensitic Transformation – ICOMAT, 14-17 June, 2005, Shanghai, China.

Sashihara, E.M., 2007, "Production and characterization of NiTi shape memory alloy by electron beam melting", Master of Science Thesis, ITA, S. J. dos Campos, São Paulo, Brazil.

Stoeckel, D., 1989, "Fabrication and properties of nickel-titanium shape memory alloy wires", Wire Journal International, pp. 30-40.

Vassileva, V., Vutova, K., Mladenov, G., 2001, "An investigation of the influence of heat transfer on crystallisation processes during electron beam melting and casting of metals", Vacuum, Vol. 62, pp. 197-201.

Vassileva, V., Mladenov, G., Vutova, K., Nikolov, T., Georgieva, E., 2005, "Oxygen removal during electron beam drip melting and refining", Vacuum, Vol. 77, pp. 429-436.

## 7. RESPONSIBILITY NOTICE

The authors are the only responsible for the printed material included in this paper.